Role of the possible $\Sigma^*(\frac{1}{2}^-)$ state in the $\Lambda p \to \Lambda p \pi^0$ reaction

Ju-Jun Xie,[1,2,3,*] Jia-Jun Wu,[4] and Bing-Song Zou[3,†]

[1]*Institute of Modern Physics, Chinese Academy of Sciences, Lanzhou 730000, China*

[2]*Research Center for Hadron and CSR Physics, Institute of Modern Physics of CAS and Lanzhou University, Lanzhou 730000, China*

[3]*State Key Laboratory of Theoretical Physics, Institute of Theoretical Physics, Chinese Academy of Sciences, Beijing 100190, China*

[4]*Physics Division, Argonne National Laboratory, Argonne, Illinois 60439, USA*

The $\Lambda p \to \Lambda p \pi^0$ reaction near threshold is studied within an effective Lagrangian method. The production process is described by single-pion and single-kaon exchange. In addition to the role played by the $\Sigma^*(1385)$ resonance of spin-parity $J^P = 3/2^+$, the effects of a newly proposed Σ^* ($J^P = 1/2^-$) state with mass and width around 1380 MeV and 120 MeV are investigated. We show that our model leads to a good description of the experimental data on the total cross section of the $\Lambda p \to \Lambda p \pi^0$ reaction by including the contributions from the possible $\Sigma^*(\frac{1}{2}^-)$ state. However, the theoretical calculations by considering only the $\Sigma^*(1385)$ resonance fail to reproduce the experimental data, especially for the enhancement close to the reaction threshold. On the other hand, it is found that the single-pion exchange is dominant. Furthermore, we also demonstrate that the angular distributions provide direct information of this reaction, hence could be useful for the investigation of the existence of the $\Sigma^*(\frac{1}{2}^-)$ state and may be tested by future experiments.

PACS number(s): 13.75.−n, 14.20.Gk, 13.30.Eg

I. INTRODUCTION

Study of the spectrum of the $\Sigma(1193)$ excited states, Σ^*, with isospin $I = 1$ and strangeness $S = -1$ is one of the most important issues in hadronic physics [1,2]. The Σ^* resonances were mostly produced and studied in K-induced reactions. Many Σ^* resonances are now cataloged by the Particle Data Group (PDG) [3]. However, our knowledge of these resonances is still very poor [1–3]. In the energy region below 2 GeV, only a few of them are well established, such as the $\Sigma^*(1385)$ of spin-parity $J^P = 3/2^+$, $\Sigma^*(1670)$ of $J^P = 3/2^-$ and $\Sigma^*(1775)$ of $J^P = 5/2^-$. The others are not well established with some even of large uncertainties on their existence. Thus, the study of the Σ^* resonance with available experimental data is necessary.

The $\Lambda p \to \Lambda p \pi^0$ reaction is a very good isospin one filter for studying Σ^* resonances decaying to $\pi\Lambda$, and provides a useful tool for testing Σ^* baryon models. In the low energy region, the first $\Sigma(1193)$ excited state, $\Sigma^*(1385)$, with strong couplings to $\pi\Lambda$ channel, should have a significant contribution to the $\Lambda p \to \Lambda p \pi^0$ reaction. The $\Sigma^*(1385)$ resonance is cataloged in the baryon decuplet of the traditional quark models that give a good description of the mass pattern and magnetic moments for the baryon ground states. However, the classical quark models still have some problems for the excited baryon resonances. The lowest spatial excited states of baryon are expected to be a N^* (uud) state with one quark in orbital angular momentum $L = 1$ state, and hence should have negative parity. But, experimentally, the lowest negative parity N^* resonance is $N^*(1535)$, which is

heavier than $\Lambda(1405)$[1] and $N^*(1440)$ which are spatial excited baryons. This is the long-standing mass reverse problem for the lowest spatial excited baryons. Recently, the pentaquark picture [6,7] provides the natural explanation for this problem [8]. Based on the pentaquark picture, a newly possible Σ^* state, $\Sigma^*(1380)$ ($J^P = 1/2^-$) was predicted around 1380 MeV [9]. Besides, another more general pentaquark model [6] without introducing explicitly diquark clusters also predicts this new Σ^* state around 1405 MeV. Obviously, it is helpful to check the correctness of pentaquark models by studying the possible $\Sigma^*(1380)$ state. Because the mass of this new Σ^* state is close to the well-established $\Sigma^*(1385)$ resonance, it will make effects in the production of $\Sigma^*(1385)$ resonance and then the analysis of the $\Sigma^*(1385)$ resonance suffers from the overlapping mass distributions and the common $\pi\Lambda$ decay mode. The possible existence of such a new $\Sigma^*(1380)$ state in J/ψ decays was pointed out in Ref. [10]. Recent studies of the $K^- p \to \Lambda \pi^+ \pi^-$ reaction have shown some evidence for the existence of the $\Sigma^*(1380)$ state and width around 1380 MeV and 120 MeV [11,12]. Furthermore, in Refs. [13,14], the role played by the new $\Sigma^*(1380)$ state in the $K\Sigma^*(1385)$ photoproduction reaction was studied, and it was shown that, apart from the existing $\Sigma^*(1385)$ resonance, the $\Sigma^*(1380)$ state possibly exists.

The $\Lambda p \to \Lambda p \pi^0$ reaction is difficult to study experimentally because of the relatively small probability that the short-lived Λ hyperon will interact with the target proton rather than decay. Hence, little is known about this reaction. There are only a few data points about its total cross section versus energy [15], which was obtained in bubble chamber measurements. The experimental results show a strong near

---

*xiejujun@impcas.ac.cn

†zoubs@itp.ac.cn

[1]It is worthy to mention that within the unitary chiral approaches, the $N^*(1535)$ resonance and two $\Lambda(1405)$ states are dynamically generated from the meson-baryon chiral interaction [4,5].

threshold enhancement. The $\Sigma^*(1385)$ resonance with spin-parity $3/2^+$ decays to $\pi\Lambda$ in relative P wave and is suppressed at low energies. To reproduce the near threshold enhancement for the $\Lambda p \to \Lambda p\pi^0$ reaction, a natural source could be some $J^P = 1/2^-$, Σ^* resonance(s) at low energy decay to $\pi\Lambda$ in relative S wave. Following the logic, in addition to the $\Sigma^*(1385)$ resonance, we study the role played by the possible $\Sigma^*(1380)$ state in the $\Lambda p \to \Lambda p\pi^0$ reaction by using the effective Lagrangian method. The production process is described by single-pion and single-kaon exchange. Furthermore, the Λp final state interaction (FSI) close to threshold is very strong and we also take it into account. It is shown that the existence of the $\Sigma^*(1380)$ state can also be tested in the $\Lambda p \to \Lambda p\pi^0$ reaction.

In the next section, we will show the formalism and ingredients in our calculation, then numerical results and discussions are presented in Sec. III. A short summary is given in the last section.

II. FORMALISM AND INGREDIENTS

The effective Lagrangian method is an important theoretical tool in describing the various processes around the resonance region. But, since only the tree diagrams are considered, thus the total scattering amplitudes are not consistent with the unitary requirements, which, in principle, is important for extracting the parameters of the nucleon resonances from the analysis of the experimental data [16,17], especially for those reactions involving many intermediate couple channels and three-particle final states [18,19]. In addition, it is known that it is difficult to really keep the unitary in the three bodies case, which need to include the complex loop diagrams [19–21]. Furthermore, the extracted rough parameters for the major resonances still provide useful information, hence we will leave it to further studies. Nevertheless, our model used in the present work can give a reasonable description of the experimental data for the $\Lambda p \to \Lambda p\pi^0$ reaction in the considered energy region, and our calculation offers some important clues for the mechanisms of the $\Lambda p \to \Lambda p\pi^0$ reaction and makes a first effort to study the role of possible $\Sigma^*(1380)$ state in relevant reaction.

In this section, we introduce the theoretical formalism and ingredients to study the $\Lambda p \to \Lambda p\pi^0$ reaction by using the effective Lagrangian method. In the following equations, we use Σ_1^* and Σ_2^*, which denote the $\Sigma^*(1385)$ resonance and possible $\Sigma^*(1380)$ state, respectively.

A. Feynman diagrams and effective interaction Lagrangian densities

To study the reaction of $\Lambda p \to \Lambda p\pi^0$, first we investigate the possible reaction's mechanisms. In the reaction at threshold, we consider the processes, shown in Fig. 1, involving the exchange of π [Fig. 1(a), (d)] and K [Fig. 1(b), (c) and (e)] mesons as the dominant contributions. It is also assumed that the production of the $\pi^0\Lambda$ passes mainly through the decay of the $\Sigma(1193)$, $\Sigma^*(1385)$ and the possible $\Sigma^*(1380)$ state as shown in Fig. 1(a), (b), and (d). The contributions from the nucleon pole are also considered as shown in Fig. 1(c) and (e).
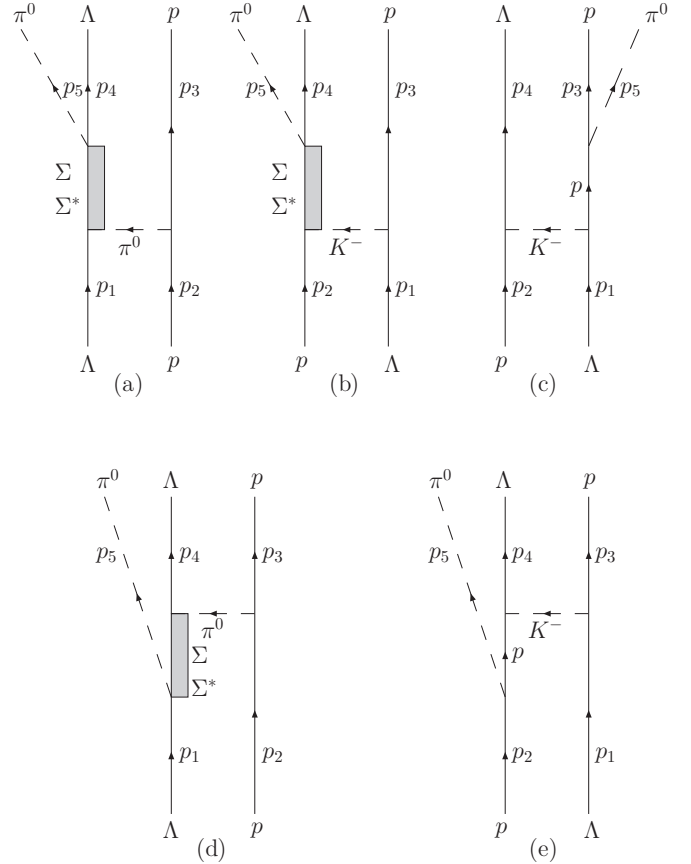

FIG. 1. Feynman diagrams for the $\Lambda p \to \Lambda p\pi^0$ reaction.

To compute the contributions of those terms shown in Fig. 1, we use the interaction Lagrangian densities as in Refs. [11,12,22–25]:

$$\mathcal{L}_{\pi NN} = -\frac{g_{\pi NN}}{2m_N}\bar{N}\gamma_5\gamma_\mu\vec{\tau}\cdot\partial^\mu\vec{\pi}N, \tag{1}$$

$$\mathcal{L}_{KN\Lambda} = -\frac{g_{KN\Lambda}}{m_N+m_\Lambda}\bar{\Lambda}\gamma_5\gamma_\mu\partial^\mu KN + \text{H.c.}, \tag{2}$$

$$\mathcal{L}_{\pi\Lambda\Sigma} = -\frac{g_{\pi\Lambda\Sigma}}{m_\Lambda+m_\Sigma}\bar{\Lambda}\gamma_5\gamma_\mu\partial^\mu\vec{\pi}\cdot\vec{\Sigma} + \text{H.c.}, \tag{3}$$

$$\mathcal{L}_{KN\Sigma} = -\frac{g_{KN\Sigma}}{m_N+m_\Sigma}\bar{N}\gamma_5\gamma_\mu\partial^\mu K\vec{\tau}\cdot\vec{\Sigma} + \text{H.c.}, \tag{4}$$

$$\mathcal{L}_{\pi\Lambda\Sigma_1^*} = \frac{g_{\pi\Lambda\Sigma_1^*}}{m_\pi}\bar{\Sigma}_1^{*\mu}(\vec{\tau}\cdot\partial_\mu\vec{\pi})\Lambda + \text{H.c.}, \tag{5}$$

$$\mathcal{L}_{KN\Sigma_1^*} = \frac{g_{KN\Sigma_1^*}}{m_K}\bar{\Sigma}_1^{*\mu}(\partial_\mu K)N + \text{H.c.}, \tag{6}$$

$$\mathcal{L}_{\pi\Lambda\Sigma_2^*} = g_{\pi\Lambda\Sigma_2^*}\bar{\Sigma}_2^*\vec{\tau}\cdot\vec{\pi}\Lambda + \text{H.c.}, \tag{7}$$

$$\mathcal{L}_{KN\Sigma_2^*} = g_{KN\Sigma_2^*}\bar{\Sigma}_2^*KN + \text{H.c.}, \tag{8}$$

where m_π and m_K are the masses of pion and kaon, respectively. The $\Sigma_1^{*\mu}$ and Σ_2^* are the fields for the $\Sigma^*(1385)$ resonance with spin-$\frac{3}{2}$ and $\Sigma^*(1380)$ state with spin-$\frac{1}{2}$, respectively.

The coupling constant for the πNN vertex is taken to be $g_{\pi NN} = 13.45$, while the coupling constants $g_{KN\Lambda} = -13.98$,

$g_{\pi\Lambda\Sigma} = 9.32$, and $g_{KN\Sigma} = 2.69$ are obtained from the SU(3) flavor symmetry. And these values have also been used in previous works [24–27] for studying different processes.

For the coupling constant $g_{\pi\Lambda\Sigma^*(1385)}$, it can be determined from the experimentally observed partial decay width of $\Sigma^*(1385) \to \pi\Lambda$. With the effective interaction Lagrangian described by Eq. (5), the partial decay width $\Gamma_{\Sigma^*(1385)\to\pi\Lambda}$ can be easily calculated. The coupling constant are related to the partial decay width as[2]

$$\Gamma_{\Sigma_1^* \to \pi\Lambda} = \frac{g_{\pi\Lambda\Sigma_1^*}^2}{12\pi} \frac{\left|\overrightarrow{p}_\Lambda^{\,\mathrm{c.m.}}\right|^3 (E_\Lambda + m_\Lambda)}{m_\pi^2 M_{\Sigma_1^*}} \quad (9)$$

with

$$E_\Lambda = \frac{M_{\Sigma_1^*}^2 + m_\Lambda^2 - m_\pi^2}{2M_{\Sigma_1^*}}, \quad (10)$$

$$\left|\overrightarrow{p}_\Lambda^{\,\mathrm{c.m.}}\right| = \sqrt{E_\Lambda^2 - m_\Lambda^2}. \quad (11)$$

For the $KN\Sigma^*(1385)$ coupling, it can be related with the $\pi N\Delta$ coupling by the SU(3) flavor symmetry relation [22,26]

$$\frac{g_{\pi N\Delta}}{m_\pi} = -\sqrt{6}\frac{g_{KN\Sigma_1^*}}{m_K}. \quad (12)$$

With the $\pi N\Delta$ coupling constant, $g_{\pi N\Delta} = 2.18$ obtained from the Δ decay width $\Gamma_{\Delta\to\pi N} = 120$ MeV,[3] we obtain $g_{KN\Sigma^*(1385)} = -3.19$ from the above equation.

Finally, we take the coupling constant $g_{\pi\Lambda\Sigma^*(1380)}$ as 2.12 [14] which is obtained by assuming the fitted results 120 MeV of the $\Sigma^*(1380)$ total decay width in Refs. [11,12] is contributed totally by the $\pi\Lambda$ channel. On the other hand, for the $KN\Sigma^*(1380)$ coupling, it is taken as 1.34, which is the fitted result of Refs. [11,12].

In evaluating the scattering amplitudes of $\Lambda p \to \Lambda p\pi^0$ reaction, we need to include the form factors because the hadrons are not point like particles. We adopt here the common scheme used in many previous works:

$$F_{\pi/K}^{NN/\Lambda}(k_{\pi/K}^2) = \frac{\Lambda_{\pi/K}^2 - m_{\pi/K}^2}{\Lambda_{\pi/K}^2 - k_{\pi/K}^2}, \quad (13)$$

$$F_{\pi/K}^{\Lambda N/\Sigma}(k_{\pi/K}^2) = \frac{\Lambda_{\pi/K}^2 - m_{\pi/K}^2}{\Lambda_{\pi/K}^2 - k_{\pi/K}^2}, \quad (14)$$

$$F_{\pi/K}^{\Sigma^*\Lambda/N}(k_{\pi/K}^2) = \left(\frac{\Lambda_{\pi/K}^{*2} - m_{\pi/K}^2}{\Lambda_{\pi/K}^{*2} - k_{\pi/K}^2}\right)^n, \quad (15)$$

———

[2]With mass $M_{\Sigma^*(1385)} = 1384.57$ MeV, total decay width $\Gamma_{\Sigma^*(1385)} = 37.13$ MeV, and decay branching ratio of $\Sigma^*(1385)$, Br[$\Sigma^*(1385) \to \pi\Lambda] = 0.87$, we obtain the coupling constant, $g_{\pi\Lambda\Sigma^*} = 1.26$.

[3]With the Lagrangian, $\mathcal{L}_{\pi N\Delta} = \frac{g_{\pi N\Delta}}{m_\pi} \bar{\Delta}^\mu (\vec{\tau} \cdot \partial_\mu \vec{\pi})N + \mathrm{H.c.}$, we obtain for the $\Delta \to \pi N$ decay width

$$\Gamma_{\Delta\to\pi N} = \frac{g_{\pi N\Delta}^2}{12\pi m_\pi^2} \frac{(E_N + m_N)(E_N^2 - m_N^2)^{3/2}}{M_\Delta},$$

where $E_N = \frac{M_\Delta^2 + m_N^2 - m_\pi^2}{2M_\Delta}$ is the nucleon energy in the Δ rest frame.

$$F_{\Sigma^*}(q_{\Sigma^*}^2) = \left[\frac{\Lambda_{\Sigma^*}^4}{\Lambda_{\Sigma^*}^4 + (q_{\Sigma^*}^2 - M_{\Sigma^*}^2)^2}\right]^n, \quad (16)$$

$$F_p(q_p^2) = \frac{\Lambda_p^4}{\Lambda_p^4 + (q_p^2 - m_p^2)^2}, \quad (17)$$

$$F_\Sigma(q_\Sigma^2) = \frac{\Lambda_\Sigma^4}{\Lambda_\Sigma^4 + (q_\Sigma^2 - m_\Sigma^2)^2}, \quad (18)$$

where $k_\pi = p_2 - p_3$ [Fig. 1(a), (d)], $k_K = p_1 - p_3$ [Fig. 1(b), (e)], $k_K = p_4 - p_2$ [Fig. 1(c)] are the four-momentum of the exchanged π^0 meson, K^- meson, while $q_{\Sigma/\Sigma^*} = p_4 + p_5$ [Fig. 1(a), (b)], $q_{\Sigma/\Sigma^*} = p_1 - p_5$ [Fig. 1(d)], and $q_p = p_3 + p_5$ [Fig. 1(c)], $q_p = p_2 - p_5$ [Fig. 1(e)] are the four-momentum of the Σ^* resonances and the nucleon pole. On the other hand, we take $n = 2$ for $\Sigma^*(1385)$ resonance and $n = 1$ for $\Sigma^*(1380)$ state. The $\Lambda_{\pi/K}$, $\Lambda_{\pi/K}^*$, and Λ_{Σ^*} are cut-off parameters, which are taken as commonly used ones: $\Lambda_\pi = \Lambda_K = 1.3$ GeV, $\Lambda_\pi^* = \Lambda_K^* = \Lambda_{\Sigma^*} = \Lambda_p = \Lambda_\Sigma = 0.8$ GeV.

B. Scattering amplitudes

To get the invariant scattering amplitudes for the reaction $\Lambda p \to \Lambda p\pi^0$, we need also the propagators for π and K mesons, nucleon pole, $\Sigma(1193)$ pole, $\Sigma^*(1380)$ state, and $\Sigma^*(1385)$ resonances,[4]

$$G_{\pi/K}(k_{\pi/K}^2) = \frac{i}{k_{\pi/K}^2 - m_{\pi/K}^2}, \quad (19)$$

$$G_p(q_p) = i\frac{\slashed{q}_p + m_p}{q_p^2 - m_p^2}, \quad (20)$$

$$G_\Sigma(q_\Sigma) = i\frac{\slashed{q}_\Sigma + m_\Sigma}{q_\Sigma^2 - m_\Sigma^2}, \quad (21)$$

$$G_{\Sigma_2^*}(q_{\Sigma_2^*}) = i\frac{\slashed{q}_{\Sigma_2^*} + M_{\Sigma_2^*}}{q_{\Sigma_2^*}^2 - M_{\Sigma_2^*}^2 + iM_{\Sigma_2^*}\Gamma_{\Sigma_2^*}}, \quad (22)$$

$$G_{\Sigma_1^*}^{\mu\nu}(q_{\Sigma_1^*}) = i\frac{\slashed{q}_{\Sigma_1^*} + M_{\Sigma_1^*}}{D}P^{\mu\nu} \quad (23)$$

with

$$D = s - M_{\Sigma_1^*}^2 + iM_{\Sigma_1^*}\Gamma_{\Sigma_1^*}, \quad (24)$$

$$P^{\mu\nu} = -g^{\mu\nu} + \frac{1}{3}\gamma^\mu\gamma^\nu + \frac{2}{3M_{\Sigma_1^*}^2}q_{\Sigma_1^*}^\mu q_{\Sigma_1^*}^\nu$$
$$+ \frac{1}{3M_{\Sigma_1^*}}(\gamma^\mu q_{\Sigma_1^*}^\nu - \gamma^\nu q_{\Sigma_1^*}^\mu), \quad (25)$$

where $M_{\Sigma_1^*}$ ($M_{\Sigma_2^*}$) and $\Gamma_{\Sigma_1^*}$ ($\Gamma_{\Sigma_2^*}$) are the mass and total decay width of the $\Sigma^*(1385)$ [$\Sigma^*(1380)$] resonance, respectively. We take $M_{\Sigma_2^*}$ and $\Gamma_{\Sigma_2^*}$ as 1380 MeV and 120 MeV which were used in Refs. [11,12].

———

[4]It is worth noting that we take $\Gamma_{\Sigma_{1,2}^*} = 0$ for the calculation of Fig. 1(d) since $q_{\Sigma_{1,2}^*}^2 < 0$ in this case.

Then, the full invariant scattering amplitude of the $\Lambda p \to \Lambda p \pi^0$ reaction is composed of five parts corresponding to the diagrams shown in Fig. 1:

$$\mathcal{M} = \mathcal{M}_a^{\Sigma, \Sigma_1^*, \Sigma_2^*} + \mathcal{M}_b^{\Sigma, \Sigma_1^*, \Sigma_2^*} + \mathcal{M}_c^p$$
$$+ M_d^{\Sigma, \Sigma_1^*, \Sigma_2^*} + \mathcal{M}_e^p. \tag{26}$$

Each of the above amplitudes can be obtained straightforwardly with the effective couplings and following the Feynman rules. Here we give explicitly the amplitude $\mathcal{M}_a$ for the $\Sigma^*(1380)$ state, as an example,

$$\mathcal{M}_a^{\Sigma_2^*} = g_{\pi NN} g_{\pi \Lambda \Sigma_2^*}^2 F_\pi^{NN}(k_\pi^2) F_\pi^{\Sigma_2^* \Lambda}(k_\pi^2) F_{\Sigma_2^*}(q_{\Delta^*}^2)$$
$$\times \bar{u}(p_4, s_4) G_{\Sigma_2^*}(q_{\Sigma_2^*}) u(p_1, s_1) G_\pi(k_\pi^2)$$
$$\times \bar{u}(p_3, s_3) \gamma_5 u(p_2, s_2), \tag{27}$$

where $s_i(i = 1,2,3,4)$ and $p_i(i = 1,2,3,4)$ represent the spin projection and four-momenta of the initial and final Λ hyperons and protons, respectively.

C. Final state interaction

To study the possible influence from the Λp FSI, we include it in our calculation by introducing a FSI enhancement factor $|C_{\text{FSI}}|^2$,

$$|\mathcal{M}|^2 \to |\mathcal{M}|^2 |C_{\text{FSI}}|^2, \tag{28}$$

where the correction C_{FSI} is given as

$$C_{\text{FSI}} = \frac{q - i\beta}{q + i\alpha}, \tag{29}$$

where q is the internal momentum of Λp subsystem, and the α and β are related to the spin-averaged scattering lengths $\bar{a}$ and the effective ranges $\bar{r}$ of the low energy S-wave scattering,

$$\alpha = \frac{1}{\bar{r}}\left(1 - \sqrt{1 - \frac{2\bar{r}}{\bar{a}}}\right), \quad \beta = \frac{1}{\bar{r}}\left(1 + \sqrt{1 - \frac{2\bar{r}}{\bar{a}}}\right) \tag{30}$$

with $\bar{a} = -1.75$ and $\bar{r} = 3.43$ obtained in Refs. [28–31], we get $\alpha = -70.1$ MeV and $\beta = 185.1$ MeV.

To end this section, it is worth mentioning that, in general, the Λp interaction is spin-dependent. Thus, to analyze the low energy elastic $\Lambda p \to \Lambda p$ transition cross section, we need four parameters: scattering length a_s and effective range r_s for the spin of Λp system $S_{\Lambda p} = 0$; scattering length a_t and effective range r_t for $S_{\Lambda p} = 1$. However, the current lower energy experimental data on the $\Lambda p \to \Lambda p$ reaction and $pp \to \Lambda p K^+$ reaction only support the determination of a spin-averaged scattering length $\bar{a}$ and effective range $\bar{r}$ [28–31]. Indeed, as pointed in Ref. [31], only two parameters in the Λp interaction are enough to reproduce the current experimental data on low energy Λp scattering.

III. NUMERICAL RESULTS AND DISCUSSION

With the formalism and ingredients given above, the calculations of the differential and total cross sections for
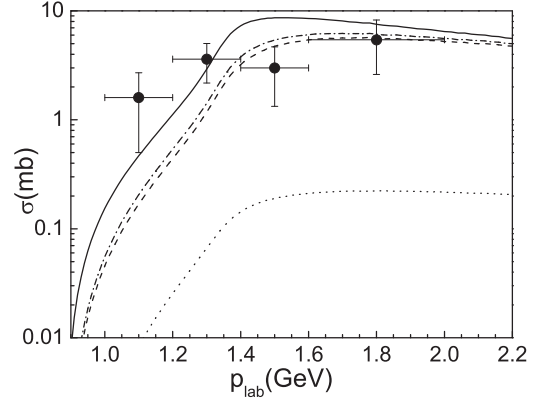

FIG. 2. Total cross sections vs the beam momentum p_{lab} for the $\Lambda p \to \Lambda p \pi^0$ reaction. The experimental data are taken from Ref. [15]. The dashed and dotted curves stand for the contributions of π^0 and K^- exchange, respectively, while the solid (with Λp FSI) and dash-dotted (without Λp FSI) are their total contributions.

$\Lambda p \to \Lambda p \pi^0$ are straightforward:

$$d\sigma(\Lambda p \to \Lambda p \pi^0)$$
$$= \frac{1}{4} \frac{m_\Lambda m_p}{F} \sum_{s_1, s_2} \sum_{s_3, s_4} |\mathcal{M}|^2 \frac{m_p d^3 p_3}{E_3} \frac{m_\Lambda d^3 p_4}{E_4}$$
$$\times \frac{d^3 p_5}{2 E_5} \delta^4(p_1 + p_2 - p_3 - p_4 - p_5), \tag{31}$$

with the flux factor

$$F = (2\pi)^5 \sqrt{(p_1 \cdot p_2)^2 - m_\Lambda^2 m_p^2}. \tag{32}$$

The theoretical results of the total cross section for beam energies p_{lab} from just above the production threshold 0.9 GeV to 2.2 GeV are shown in Fig. 2. In this figure we have investigated the role of various meson exchange processes in describing the total cross section. The dashed and dotted lines stand for contributions from π^0 and K^- exchange, respectively. Their total contributions are shown by the dash-dotted line, while the results with the Λp FSI are shown by the solid line. It is found that Λp FSI enhance the total cross section by a factor 3 close to reaction threshold. Thus the Λp FSI is indeed making a significant effect at very low energies. But it does not change the basic shape of the curve very much. Besides, from Fig. 2, we can see that the contribution from the π^0 meson exchange is predominant in the whole considered energy region, and the contribution from the K^- meson exchange is rather small and can be negligible. For comparison, we also show the experimental data [15] in Fig. 2, from which we can see that the measured total cross sections are reproduced reasonably well by our model calculations (solid line).

The relative importance of the contributions of each intermediate resonance to the $\Lambda p \to \Lambda p \pi^0$ reaction is studied in Fig. 3, where the contributions of the $\Sigma^*(1385)$ resonance, $\Sigma^*(1380)$ state, nucleon pole, and $\Sigma(1193)$ pole to the energy dependence of the total cross section are shown by dashed, dotted, dash-dotted, and dash-dot-dotted curves, respectively.
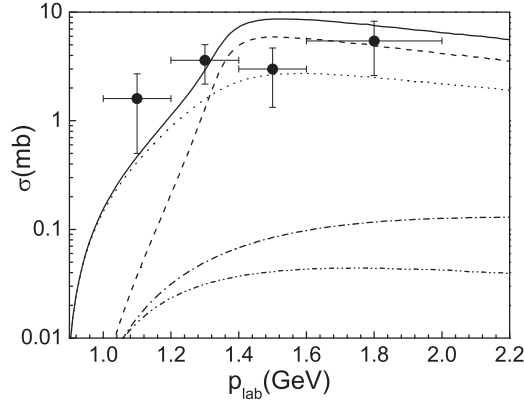
FIG. 3. Contributions of $\Sigma^*(1385)$ resonance (dashed line), $\Sigma^*(1380)$ state (dotted line), nucleon pole (dash-dotted line), and $\Sigma(1193)$ pole (dash-dot-dotted line) to the total cross sections vs the beam momentum p_{lab} for the $\Lambda p \to \Lambda p \pi^0$ reaction. Their total contribution is shown by solid line. The experimental data are taken from Ref. [15].

Their total contribution is depicted by the solid line. It is clear that the contributions from the $\Sigma^*(1380)$ state and $\Sigma^*(1385)$ resonance dominate the total cross section at beam momenta below and above 1.3 GeV, respectively, while the contributions of nucleon and $\Sigma(1193)$ pole are small and can be neglected.

As mentioned in the Introduction, the $\Sigma^*(1385)$ resonance with spin-parity $3/2^+$ decays to $\pi\Lambda$ in relative P wave and is suppressed at low energies. It cannot reproduce the near threshold enhancement for the $\Lambda p \to \Lambda p \pi^0$ reaction. On the contrary, the possible $\Sigma^*(1380)$ state with $J^P = 1/2^-$ is decaying to $\pi\Lambda$ in relative S wave, which will give enhancement at the near threshold. As we can see in Fig. 3, thanks to the contribution from $\Sigma^*(1380)$ state, we can reproduce the experimental data for all of the beam energies. Thus, we find a natural source for the near threshold enhancement of the $\Lambda p \to \Lambda p \pi^0$ reaction coming from the possible $\Sigma^*(1380)$ state which decays to $\pi\Lambda$ in the S wave.

In addition to the total cross sections, we also compute the differential cross sections for $\Lambda p \to \Lambda p \pi^0$ reaction, namely the angular distributions of all final-state particles in the overall center-of-mass frame (CMS), as well as distributions in both the Gottfried-Jackson and helicity frames as introduced in Ref. [32]. Like Dalitz plots, the helicity angle distributions provide insight into the three-body final state. While the information contained in the Gottfried-Jackson angle distributions is complementary to that of a Dalitz plot, as this angular distribution can give insight into the scattering process, especially concerning the involved partial waves.

The corresponding theoretical results at $p_{\mathrm{lab}} = 1.2$ GeV, where the contribution of the $\Sigma^*(1380)$ state is dominant, are shown in Fig. 4.[5] For comparison, we also show our theoretical predictions in Fig. 5 at $p_{\mathrm{lab}} = 1.5$ GeV, where the contribution of the $\Sigma^*(1385)$ resonance is dominant. In those figures, the
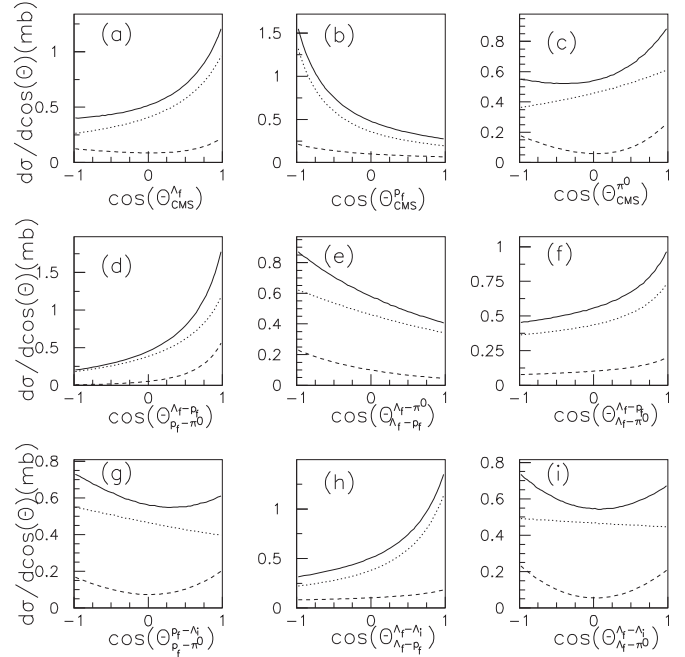
---

[5]The Λ_i (Λ_f) and p_i (p_f) stand for the initial (final) Λ hyperon and proton, respectively.

FIG. 4. Angular differential cross sections for the $\Lambda p \to \Lambda p \pi^0$ reaction in CMS [(a) $\Theta_{\mathrm{CMS}}^{\Lambda_f}$, (b) $\Theta_{\mathrm{CMS}}^{p_f}$, (c) $\Theta_{\mathrm{CMS}}^{\pi^0}$], helicity [(d) $\Theta_{p_f-\pi^0}^{\Lambda_f-p_f}$, (e) $\Theta_{\Lambda_f-p_f}^{\Lambda_f-\pi^0}$, (f) $\Theta_{\Lambda_f-\pi^0}^{\Lambda_f-p_f}$], and Gottfried-Jackson [(g) $\Theta_{p_f-\pi^0}^{p_f-\Lambda_i}$, (h) $\Theta_{\Lambda_f-p_f}^{\Lambda_f-\Lambda_i}$, (i) $\Theta_{\Lambda_f-\pi^0}^{\Lambda_f-\Lambda_i}$] reference frames. The dashed and solid curves stand for the contributions of the $\Sigma^*(1385)$ and $\Sigma^*(1380)$, respectively. The results are obtained at $p_{\mathrm{lab}} = 1.2$ GeV.

dashed and dotted curves are obtained with the contributions from $\Sigma^*(1385)$ resonance and $\Sigma^*(1380)$ state, respectively. The solid lines stand for their total contributions.

In Figs. 4, 5(a), (b), and (c), we show the final particles Λ, p, and π^0 angular distributions in the CMS, respectively. The results obtained in the helicity frame with respect to the angle, Θ_{c-d}^{a-b}, which represents the angel between particles "a" and "b" in the "c" and "d" reference frame (see more details in Refs. [32,33]), are shown in Figs. 4, 5(d), (e), and (f), while Figs. 4, 5(g), (h), and (i) depict the distributions of the Gottfried-Jackson angles. It is worth mentioning that the nine angular distributions are not kinematically independent with each other, we show here all of them for the sake of completeness.

From Figs. 4, 5, we can see that the shapes of the angular distributions of $\Sigma^*(1385)$ resonance and $\Sigma^*(1380)$ state are much different, so the existence of $\Sigma^*(1380)$ state can be tested by future experimental analysis.

IV. SUMMARY

In summary, we study the $\Lambda p \to \Lambda p \pi^0$ reaction near threshold within an effective Lagrangian method. In addition to the role played by the $\Sigma^*(1385)$ resonance (spin-parity $J^P = 3/2^+$), we study the effects of a newly proposed Σ^* ($J^P = 1/2^-$) state with mass and width around 1380 MeV and 120 MeV. We show that our model leads to a fair description of the experimental data on the total cross section of the

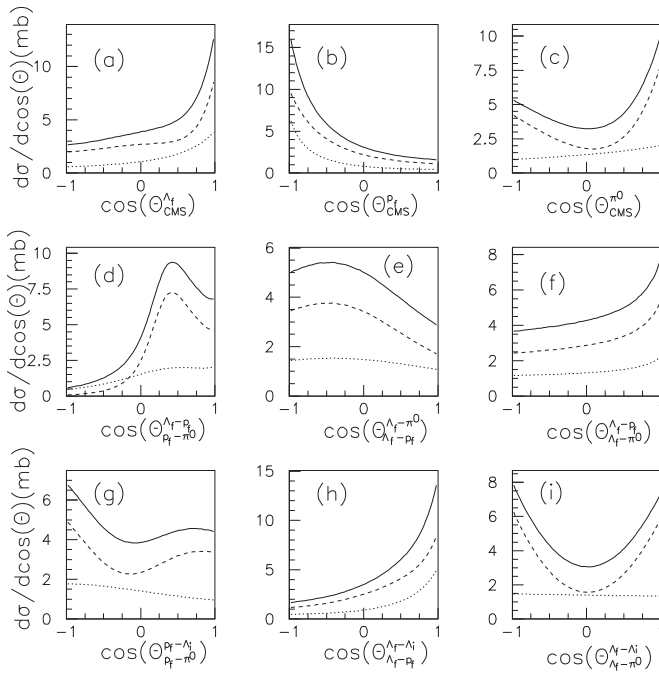FIG. 5. As in Fig. 4 but for the case of $p_{lab} = 1.5$ GeV.

$\Lambda p \rightarrow \Lambda p \pi^0$ reaction by including the contributions from the possible $\Sigma^*(\frac{1}{2}^-)$ state and the strong Λp FSI.

The $\Sigma^*(1385)$ resonance cannot reproduce the near threshold enhancement for the $\Lambda p \rightarrow \Lambda p \pi^0$ reaction because it decays to $\pi \Lambda$ in relative P wave and is suppressed at low energies. On the contrary, the newly $\Sigma^*(1380)$ state decays to $\pi \Lambda$ in relative S wave, and can describe the near-threshold enhancement fairly well, which indicate that the $\Lambda p \rightarrow \Lambda p \pi^0$ data support the existence of this $\Sigma^*(1380)$ state, and more accurate data for this reaction can be used to improve our knowledge on the $\Sigma^*(1380)$ properties. Our present calculation offers some important clues for the mechanisms of the $\Lambda p \rightarrow \Lambda p \pi^0$ reaction and makes a first effort to study the role of the $\Sigma^*(1380)$ state in a relevant reaction.

[1] E. Klempt and J.-M. Richard, Rev. Mod. Phys. **82**, 1095 (2010).
[2] V. Crede and W. Roberts, Rep. Prog. Phys. **76**, 076301 (2013).
[3] J. Beringer *et al.* (Particel Data Group), Phys. Rev. D **86**, 010001 (2012).
[4] T. Inoue, E. Oset, and M. J. Vicente Vacas, Phys. Rev. C **65**, 035204 (2002).
[5] D. Jido, J. A. Oller, E. Oset, A. Ramos, and U. G. Meissner, Nucl. Phys. A **725**, 181 (2003).
[6] C. Helminen and D. O. Riska, Nucl. Phys. A **699**, 624 (2002).
[7] R. L. Jaffe and F. Wilczek, Phys. Rev. Lett. **91**, 232003 (2003).
[8] B. S. Zou, Eur. Phys. J. A **35**, 325 (2008).
[9] A. Zhang, Y. R. Liu, P. Z. Huang, W. Z. Deng, X. L. Chen, and S.-L. Zhu, High Energy Phys. Nucl. Phys. **29**, 250 (2005).
[10] B. S. Zou, Int. J. Mod. Phys. A **21**, 5552 (2006).
[11] J.-J. Wu, S. Dulat, and B. S. Zou, Phys. Rev. D **80**, 017503 (2009).
[12] J.-J. Wu, S. Dulat, and B. S. Zou, Phys. Rev. C **81**, 045210 (2010).
[13] P. Gao, J.-J. Wu, and B. S. Zou, Phys. Rev. C **81**, 055203 (2010).
[14] Y.-H. Chen and B. S. Zou, Phys. Rev. C **88**, 024304 (2013).
[15] J. A. Kadyk, G. Alexander, J. H. Chan, P. Gaposchkin, and G. H. Trilling, Nucl. Phys. B **27**, 13 (1971).
[16] H. Kamano, B. Julia-Diaz, T.-S. H. Lee, A. Matsuyama, and T. Sato, Phys. Rev. C **80**, 065203 (2009).
[17] N. Suzuki, B. Julia-Diaz, H. Kamano, T.-S. H. Lee, A. Matsuyama, and T. Sato, Phys. Rev. Lett. **104**, 042302 (2010).
[18] H. Kamano, B. Julia-Diaz, T.-S. H. Lee, A. Matsuyama, and T. Sato, Phys. Rev. C **79**, 025206 (2009).
[19] H. Kamano, S. X. Nakamura, T. S. H. Lee, and T. Sato, Phys. Rev. D **84**, 114019 (2011).
[20] A. Martinez Torres, K. P. Khemchandani, U.-G. Meissner, and E. Oset, Eur. Phys. J. A **41**, 361 (2009).
[21] A. Martinez Torres, K. P. Khemchandani, and E. Oset, Phys. Rev. C **79**, 065207 (2009).
[22] Y. Oh, C. M. Ko, and K. Nakayama, Phys. Rev. C **77**, 045204 (2008).
[23] P. Gao, J. Shi, and B. S. Zou, Phys. Rev. C **86**, 025201 (2012).
[24] J.-J. Xie, B.-C. Liu, and C.-S. An, Phys. Rev. C **88**, 015203 (2013).
[25] J.-J. Xie, E. Wang, and B.-S. Zou, Phys. Rev. C **90**, 025207 (2014).
[26] M. Doring, C. Hanhart, F. Huang, S. Krewald, U.-G. Meissner, and D. Ronchen, Nucl. Phys. A **851**, 58 (2011).
[27] J.-J. Xie and B.-C. Liu, Phys. Rev. C **87**, 045210 (2013).
[28] F. Hinterberger and A. Sibirtsev, Eur. Phys. J. A **21**, 313 (2004).
[29] A. Sibirtsev, J. Haidenbauer, H.-W. Hammer, and S. Krewald, Eur. Phys. J. A **27**, 269 (2006).
[30] A. Sibirtsev, J. Haidenbauer, H.-W. Hammer, and U.-G. Meissner, Eur. Phys. J. A **29**, 363 (2006).
[31] J.-J. Xie, H.-X. Chen, and E. Oset, Phys. Rev. C **84**, 034004 (2011).
[32] M. Abdel-Bary *et al.* (COSY-TOF Collaboration), Eur. Phys. J. A **46**, 27 (2010); **46**, 435(E) (2010).
[33] G. Agakishiev *et al.* (HADES Collaboration), Phys. Rev. C **85**, 035203 (2012).